

## Evidence for Electrical Coupling in the SubCoeruleus (SubC) Nucleus

David S. Heister, Abdallah Hayar, Amanda Charlesworth, Charlotte Yates, Yi-Hong Zhou, and Edgar Garcia-Rill

Center for Translational Neuroscience, Department of Neurobiology and Developmental Sciences, University of Arkansas for Medical Sciences, Little Rock, Arkansas

Submitted 15 December 2006; accepted in final form 3 January 2007

**Heister DS, Hayar A, Charlesworth A, Yates C, Zhou Y-H, Garcia-Rill E.** Evidence for electrical coupling in the SubCoeruleus (SubC) nucleus. *J Neurophysiol* 97: 3142–3147, 2007. First published January 10, 2007; doi:10.1152/jn.01316.2006. SubCoeruleus (SubC) neurons, which are thought to modulate rapid-eye-movement (REM) sleep, were recorded in brain stem slices from 7- to 20-day rats and found to manifest spikelets, indicative of electrical coupling. Spikelets occurred spontaneously or could be induced by superfusion of the cholinergic agonist carbachol. Whole cell recordings revealed that carbachol induced membrane oscillations and spikelets in the theta frequency range in SubC neurons in the presence of fast synaptic blockers. Electrical coupling in neurons is mediated by the gap junction protein connexin 36 (Cx 36). We found that Cx 36 gene expression and protein in the mesopontine tegmentum decreased during development. Cx 36 protein levels specifically in the SubC decreased in concert with the developmental decrease in REM sleep. The presence of electrical coupling in the SubC introduces a novel potential mechanism of action for the regulation of sleep-wake states.

### INTRODUCTION

Early work established that electrical stimulation of the reticular activating system (RAS) in the region of the pedunculo-pontine nucleus (PPN) induced desynchronization of the electroencephalogram (EEG), similar to that seen during waking and rapid-eye-movement (REM) sleep (Moruzzi and Magoun 1949). The PPN contains cholinergic and noncholinergic neurons, some of which show increased firing during waking and REM sleep in the cat (Sakai et al. 1990; Steriade et al. 1990a,b) and rat (Datta and Siwek 2002). The PPN sends widespread projections throughout the pontomedullary reticular formation (Reese et al. 1995), including the anterior pontine region (Datta et al. 1998; Mitani et al. 1988; Shiromani et al. 1988). Injections of the cholinergic agonist carbachol (CAR) into this region induce a REM sleep-like state, including atonia and ponto-geniculo-occipital (PGO) waves (Baghdoyan et al. 1984; Datta et al. 1998; Marks et al. 1980; Mitler and Dement 1974; Mouret et al. 1967; Morrison 1988; Vanni-Mercier and Debilly 1989; Yamamoto et al. 1990). Lesion of this pontine area, termed the SubCoeruleus (SubC), can produce REM sleep without atonia (Jouvet and Delorme 1965; Karlsson et al. 2005; Mouret et al. 1967; Morrison 1988; Sanford et al. 1994), or REM sleep without P-waves, the rat equivalent of PGO waves (Mavanji et al. 2004). Neurons in this region are depolarized or hyperpolarized by muscarinic agonists (Gerber et al. 1991; Greene et al. 1989; Imon et al. 1996; Stevens et al.

1993). Recent comprehensive studies of SubC cells reported excitation by CAR of cells with low-threshold spikes (LTS), and of cells inhibited by CAR, some with LTS currents (Brown et al., 2006). A recent report found that PPN lesions decreased waking and increased REM sleep and posited a flip-flop switch between the central gray as a REM-off center interacting with a REM-on center located in the PPN (REM-on and wake-REM-on cells have been described in PPN) and extending to the SubC (Lu et al. 2006). These two centers were found to contain GABA neurons that were proposed to inhibit each other to create the switch, implicating SubC neurons in the control of REM sleep (Lu et al. 2006). However, others previously reported that PPN lesions decreased REM sleep (Deurveilher and Hennevin 2001; Webster and Jones 1988), and no REM-off cell activity has been reported in the central gray to date.

During our study of SubC neurons, we detected spikelets, indicative of the presence of electrical coupling in some of these cells. Frequently, electrical coupling is present in GABAergic neurons (Connors and Long 2004) and is mediated by the neuronal gap junction protein Connexin 36 (Cx 36) (Srinivas et al. 1999). Because gap junctions are developmentally regulated, we investigated Cx 36 gene expression and protein levels in relation to the developmental decrease in REM sleep known to occur between birth and puberty in man (Roffwarg et al. 1966) but between 10 and 30 days in the rat (Jouvet-Mounier et al. 1970). We describe electrophysiological, pharmacological and molecular evidence suggestive of the presence of electrical coupling in the SubC. The manifestation of electrical coupling in part of the RAS introduces a novel potential mechanism of action for the regulation of sleep-wake states.

### METHODS

Pups aged 7–20 days from adult timed-pregnant Sprague-Dawley rats (280–350 g) were anesthetized with ketamine (70 mg/kg im) until tail pinch reflex was absent. They were decapitated, and the brain was rapidly removed and cooled in oxygenated sucrose-artificial cerebrospinal fluid (sucrose-ACSF). The sucrose-ACSF consisted of (in mM) 233.7 sucrose, 26 NaHCO<sub>3</sub>, 8 MgCl<sub>2</sub>, 0.5 CaCl<sub>2</sub>, 20 glucose, 0.4 ascorbic acid, and 2 sodium pyruvate. Coronal and parasagittal sections (400  $\mu$ m) containing the SubC were cut, and slices were allowed to equilibrate in normal ACSF at room temperature for 1 h. The ACSF was composed of (in mM) 117 NaCl, 4.7 KCl, 1.2 MgSO<sub>4</sub>, 2.5 CaCl<sub>2</sub>, 2.8 NaH<sub>2</sub>PO<sub>4</sub>, 24.9 NaHCO<sub>3</sub>, and 11.5 glucose. Slices were recorded at 30°C while superfused (1.5 ml/min) with oxygenated (95% O<sub>2</sub>-5%

Address for reprint requests and other correspondence: E. Garcia-Rill, Center for Translational Neuroscience, Dept. of Neurobiology and Developmental Sciences, University of Arkansas for Medical Sciences, 4301 W. Markham St., Slot 847, Little Rock, AR, 72205 (E-mail: GarciaRillEdgar@uams.edu).

The costs of publication of this article were defrayed in part by the payment of page charges. The article must therefore be hereby marked “advertisement” in accordance with 18 U.S.C. Section 1734 solely to indicate this fact.

CO<sub>2</sub>) normal ACSF. Differential interference contrast optics was used to visualize neurons using an upright microscope (Nikon Eclipse FN-1, Nikon).

Whole cell recordings were acquired using borosilicate glass capillaries pulled on a P-97 puller (Sutter Instrument, Novato, CA) and filled with a solution of (in mM) 114 K-gluconate, 17.5 KCl, 4 NaCl, 4 MgCl<sub>2</sub>, 10 HEPES, 0.2 EGTA, 3 Mg<sub>2</sub>ATP, 0.3 Na<sub>2</sub>GTP, and 0.02% Lucifer yellow. Osmolarity was adjusted to ~270–290 mosM and pH to 7.4. The pipette resistance was 5–8 MΩ. All recordings were made using a Multiclamp 700B amplifier (Axon Instruments, Foster City, CA). Analog signals were low-pass filtered at 2 kHz (Multiclamp 700B) and digitized at 5kHz using a Digidata-1322A and pClamp9 software (Axon instruments). Off-line analyses were performed using Clampfit software (Axon Instruments). Drugs were applied to the slice via a peristaltic pump (Cole-Parmer, Vernon Hills, IL) and a three-way valve system. CAR (20–50 μM), carbenoxolone (CBX, 300 μM), 6-cyano-7-nitroquinoxaline-2, 3-dione (CNQX, 10 μM), gabazine (GAB, 10 μM), strychnine (STR, 10 μM), and (±)-2-amino-5-phosphopentanoic acid (APV, 10 μM) were all purchased from Sigma (St. Louis, MO). CNQX, APV, and GAB are termed herein as fast synaptic blockers.

For sharp electrode intracellular recordings (80–100 MΩ), pipettes were filled with 3 M potassium acetate and 1% neurobiotin. Only neurons with a resting membrane potential (RMP) more than –55 mV, action potentials (AP) >50 mV, and stable recordings were included in data analyses. In current-clamp mode, a series of hyperpolarizing and depolarizing current steps of 0.1–0.9 nA at RMP were applied to determine several membrane properties as previously described (Garcia-Rill et al. 2003).

The locations of recorded cells were determined using histological verification of neurobiotin- or Lucifer-yellow-injected cells. Most neurons were located anterior to the seventh nerve in the region of the rat brain stem termed dorsal SubC, and some were found in the more dorsal region closer to the locus coeruleus known as SubC pars alpha. Although tyrosine hydroxylase immunocytochemistry was not performed, most recordings were well ventral to the locus coeruleus and scattered tyrosine hydroxylase-positive neurons. We did not attempt to identify different morphological or neurotransmitter types due to the small sample.

In three litters, a region of the mesopontine tegmentum containing the PPN and SubC as well as locus coeruleus and posterior substantia nigra was dissected and analyzed for Cx 36 gene expression and protein levels in 7-day, 17-day, and adult rats (60 day) from each litter. To sample the SubC specifically, we cut 400-μm sagittal sections such as those used for recordings and punched (1 mm) the SubC in 10- and 30-day animals from each of four additional litters. For Cx 36 protein analysis, tissue was homogenized in RIPA buffer (50 mM Tris-Cl, pH 7.45, 150 mM NaCl 1% NP-40, 0.5% Nadeoxycholate, 0.1% SDS) with protease inhibitor cocktail (Sigma) and cell debris removed by centrifugation. Protein (50 μg/lane) was separated by SDS-PAGE and transferred onto nitrocellulose. Blots were blocked in 5% nonfat milk in TBS (Tris-buffered saline: 20 mM Tris-Cl, pH 7.5, 150 M NaCl) overnight at 4°C. Anti-Cx 36 antibodies were used at 1:250 (Invitrogen) in TBST (TBS with 0.05% Tween-20) with 1% milk, 4 h, 25°C (51p-6200 for mesopontine tegmentum, 51–6300 for SubC punches). Anti-rabbit IgG-HRP was used at 1:2,500 (Promega) in TBST for 1 h at 25°C. Proteins in were visualized using SuperSignal (Pierce) and X-ray film (mesopontine tegmentum), or Chemiglow West (Alpha Innotech) and light emission captured by a Fluorchem SP (Alpha Innotech; SubC punches). Blots were stripped with Restore (Pierce) and reprobed with antibodies against actin (CP01, Calbiochem, San Diego, CA) to verify equal protein loading. AlphaEase software was used to quantitate the amount of Cx 36 and actin protein in the SubC.

For Cx 36 mRNA expression, mesopontine tegmentum tissue was homogenized in RNA lysis buffer, and total RNA extracted using RNeasy Mini Kit (QIAGEN, Valencia, CA) following the manufac-

turer's protocol. cDNA was made from 0.2–0.5 μg RNA using poly (dT) primer and Superscript II reverse transcriptase (Invitrogen) following the manufacturer's protocol. The cDNA was diluted 20 times with 10 mM Tris.HCl (pH 7.5), and a 4-μl aliquot used to perform quantitative RT-PCR with primers and standards developed specifically for rat Cx 36 [aka gap junction protein alpha 9 (Gja9)] following procedures described previously (Zhou et al. 2005). Quantitative real-time PCR was conducted using a Roche LightCycler Instrument in 10-μl glass capillaries (Roche, Indianapolis, IN), using primers Cx36-F2 (5'–CAGCAGCACTCCACTATGAT–3') and Cx 36-R2 (5'–ACACCATTATGATCTGGAAGA C–3'), in 3.5 mM MgCl<sub>2</sub>, with the cycling parameters: 95°C, 10 s; 60°C, 5 s; 72°C, 10 s. The expression of three rat housekeeping genes (Hprt, Eno1, and Gapdh) was quantified as previously described (Iruthayanathan et al. 2005). To identify the appropriate internal control gene for normalizing Cx 36 expression in mesopontine tegmentum across age, a statistical approach was used as described previously (Zhou et al. 2003).

For comparison of data between the different groups in each experiment, measures were tested using one-factor ANOVA to conclude whether any of the factors has a significant effect on the magnitude of the variable and also whether the interaction of the factors significantly affects the variable. Differences were considered significant at values of  $P \leq 0.05$ . If statistical significance was present, the Scheffe post hoc test was used to compare between groups.

## RESULTS

Sharp electrode intracellular recordings revealed the presence of spikelets occurring spontaneously in cells from rats sampled at 7–15 days. Figure 1A shows that action potentials and low-amplitude (3–4 mV) spikelets were evident in a neuron located in the SubC. Figure 1B shows that spikelets had a similar initial rise time as action potentials in the same cell, but the waveform showed a slower decay. The frequency of observing spontaneous spikelets in SubC neurons recorded with sharp electrodes was 2/4. One of the SubC cells manifesting spikelets showed at least two cells labeled by a single intracellular injection, that is, it showed dye coupling (not shown). We investigated the possibility of inducing spikelets in SubC neurons by applying CAR. CAR administration in 9 SubC neurons induced or increased spikelet-like events in 4/9 (44%) of these cells. Figure 1C shows a lack of spontaneous spikelets in a SubC neuron; however, spikelets were induced (Fig. 1D) along with action potentials (Fig. 1E) by CAR superfusion, and they disappeared as CAR was washed out (Fig. 1F).

To better resolve the occurrence of gap junction and synaptic currents, we further investigated SubC neurons using whole cell patch-clamp recordings. A brief survey of 32 SubC cells revealed that there were 18 neurons with LTS currents, 24 neurons with  $I_A$  current, and 20 neurons with  $I_h$  current. Of these, 3/32 exhibited spontaneous spikelets, whereas another 5/32 required CAR application to induce spikelets. To investigate whether SubC neurons manifested electrical coupling, CNQX, APV, and gabazine (called hereafter “fast synaptic blockers”) were applied to block chemical synapses and neuronal activity was stimulated using CAR (20–50 μM). Recordings were carried out in voltage clamp at a holding potential of –50 mV (near resting potential for most SubC neurons) to prevent activation of voltage-dependent currents, and to record excitatory postsynaptic currents (EPSCs) as inward currents

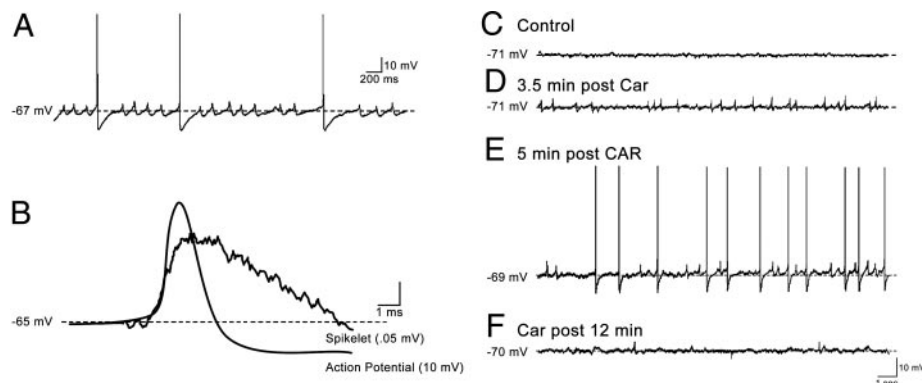


FIG. 1. Sharp electrode recordings of SubCoeruleus (SubC) cells. *A*: spiking pattern of a 12-day SubC cell exhibiting spontaneous action potentials and spikelets. *B*: superimposed recordings of a spikelet and an action potential shown at the same time scale but with different amplitude scales. Note the similar rise time between action potential and spikelet. *C*: recordings from another SubC cell (9 days) at resting membrane potential ( $-71$  mV) without spontaneous potential. *D*: recording 3.5 min after beginning of superfusion with carbachol (CAR,  $40$   $\mu$ M) showing induction of spikelets without changing the membrane potential. *E*: depolarization to  $-69$  mV induced by 5 min after the beginning of CAR superfusion showing depolarization along with action potentials and spikelets. *F*: washout of CAR showing return toward resting membrane potential, lack of action potentials, and decrease in spikelet frequency.

and inhibitory PSCs (IPSCs) as outward currents. In the presence of fast synaptic blockers, only 2 of 10 cells exhibited detectable oscillations/spikelets (3.5 and 4.0 Hz). However, additional application of CAR ( $50$   $\mu$ M) induced the appearance of membrane current oscillations/spikelets in 4 of 10 SubC cells at a frequency of  $4.4 \pm 1.2$  Hz ( $n = 4$ , range: 2.5–8 Hz, Fig. 2*A*). Spikelets and membrane current oscillations appeared to occur at the same frequency; however, occasionally such oscillations occurred without detectable spikelets. In these cases, we used power spectrum analysis to quantify the fre-

quency of spikelets/oscillations. In the presence of fast synaptic blockers and CAR, 8 of 32 (25%) cells exhibited rhythmic membrane oscillations or spikelets. The spikelets were recorded as inward currents and were distinguished from EPSCs because they appeared to have different kinetic properties. These spikelets were rhythmic events with sharp rise times and were often followed by slow outward currents thus resembling the shape of an inverted and filtered action potential, consistent with the low-pass filtering characteristics of gap junctions (Vandecasteele et al. 2005; Veruki and Hartveit 2000).

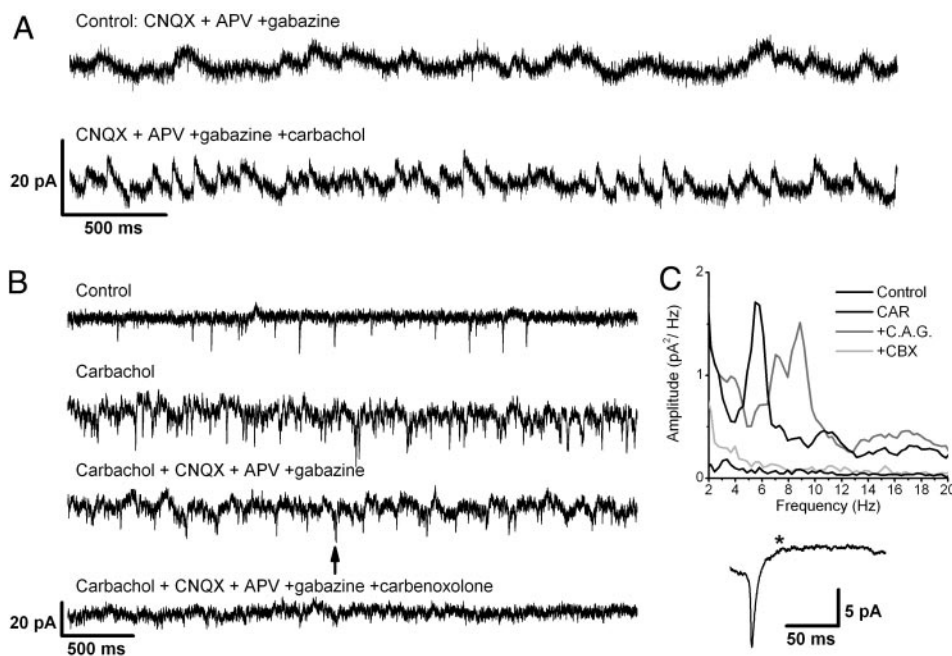


FIG. 2. CAR induces the appearance of oscillations/spikelets in SubC cells. *A*: recordings were made in voltage-clamp mode at holding potential of  $-50$  mV. Application of CAR ( $50$   $\mu$ M) in the presence of the fast synaptic blockers [6-cyano-7-nitroquinoxaline-2,3-dione (CNQX),  $10$   $\mu$ M; 2-amino-5-phosphonvaleric acid (APV),  $50$   $\mu$ M; and gabazine,  $10$   $\mu$ M], induced high-frequency membrane oscillations ( $\sim 8$  Hz) in a 10-day SubC cell. *B*: in another SubC cell (8 days), compared with control conditions (*top*), application of CAR increased the frequency of synaptic or gap junction currents (*2nd* recording). Blockade of fast synaptic currents by CNQX, APV, and gabazine, revealed gap junction currents or spikelets (*3rd* recording), and these were blocked by application of the gap junction blocker carbenoxolone ( $300$   $\mu$ M; *bottom*).  $\uparrow$ , individual spikelet. *C*: power spectrum analysis of current recordings of the same cell shown in *B* under different recording conditions [CAG: CNQX, APV, and gabazine (GAB), CBX: carbenoxolone] revealed low power in the control condition, the occurrence of oscillations/spikelets events at  $\sim 6$  Hz after CAR, which increased to  $\sim 8$  Hz in the presence of synaptic blockers with CAR but were blocked by CBX. *D*: spikelet-triggered averaging of 203 recordings in the presence of CNQX, APV, and GAB revealed the characteristic waveform of a typical spikelet with a relatively fast rise time followed by a slow anti-peak (\*).

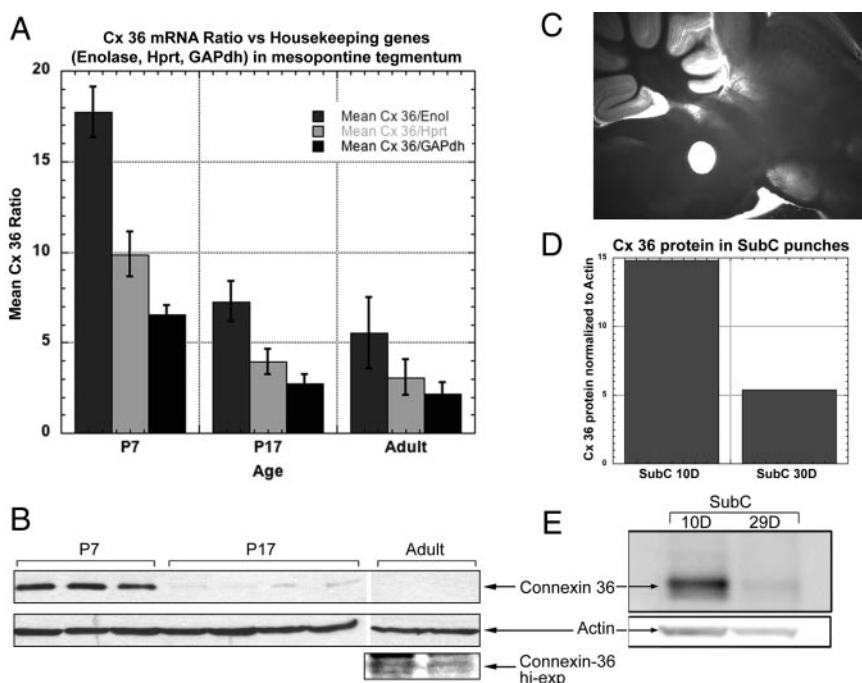


FIG. 3. Connexin 36 expression and protein levels over age. *A*: ratio of Connexin 36 (Cx 36) mRNA vs. each of 3 housekeeping genes, Enolase (dark gray), Hprt (light gray), and Gapdh (black), which did not differ from each other in developmental expression. Mean and SE of 3 mesopontine tegmenti of 7-day, 17-day, and adult rats. Note the gradual decrease in Cx 36 expression in development but with significant levels present in adults. *B*: Cx 36 protein levels in representative mesopontine tegmenti of 7-day, 17-day, and adult rats. Levels decreased gradually from 7 to 17 days to adult, such that longer exposures (Connexin-36 hi-exp) were required to visualize protein levels in adults. Blot was reprobed for actin protein levels to verify equal loading. *C*: photomicrograph of 400- $\mu$ m sagittal slice through a 30-day medial brain stem showing punched region (1 mm diam) ventral to the locus coeruleus (the punch was centered anterior to the 7th nerve but included the nerve as it descended) in the SubC region. *D*: Cx 36 protein levels were normalized to Actin in slices containing the SubC from rats from 4 litters aged 10 and 30 days. Note the decrease in protein levels across the developmental decrease in rapid-eye-movement (REM) sleep. *E*: Cx 36 protein from these pooled samples from 10 day and 30 rats normalized to Actin loading. Actin protein levels are shown to verify equal loading.

Figure 2*B* shows the effects of the gap junction blocker CBX when administered after application of CAR in the presence of the fast synaptic blockers CNQX, APV, and gabazine. CBX superfusion led to reduction or cessation of spikelets in all five cells tested. Figure 2*C* shows a power spectrum of spikelets demonstrating little power in the initial condition, induction of theta oscillations ( $\sim 6$  Hz) after CAR, increased frequency oscillations after synaptic blockers and CAR ( $\sim 8$  Hz), and a decrease in power to initial levels after the application of CBX. Figure 2*D* shows a characteristic spikelet waveform.

We further investigated whether neurons exhibiting spikelets had any characteristic voltage-dependent currents. We found that 5 of 18 (28%) cells with LTS manifested spikelets, 7 of 24 (29%) cells with  $I_A$  currents had spikelets, and 6 of 20 (30%) cells with  $I_h$  cells had spikelets. Please note that some cells had more than one type of current.

We next investigated the presence of gap junctions using molecular techniques. Because Cx 36 is a neuronal gap junction protein, we examined Cx 36 gene expression in the mesopontine tegmentum and the SubC specifically for both mRNA and protein levels. Because studies suggest a reduction of electrical coupling may occur by 14 days of age, at least in some regions (Walton and Navarrete 1991), we analyzed tissue across a wide developmental period. We first dissected the mesopontine tegmentum, omitting the colliculi, cerebellum, medulla, and midbrain anterior to the midcollicular level, in rats aged 7 days, 17 days, and adult (60 days). Figure 3*A* shows that the ratio of mRNA expression of Cx 36 compared with each of three housekeeping genes, Enolase, Hprt, and Gapdh

(the ratios of these genes against each other did not change during development), were all high at 7 days, reduced by  $>50\%$  by 17 days and by two-thirds in the adult. Figure 3*B* shows that Cx 36 protein levels were also high at 7 days, considerably decreased by 17 days and required extended exposure to be visible in the adult.

We then sampled selectively in the SubC nucleus for Cx 36 protein levels using 1-mm punches of tissue taken from 400- $\mu$ m slices (Fig. 3*C*), at later days because protein levels can lag mRNA expression levels, and across the developmental decrease in REM sleep. Figure 3*D* shows that Cx 36 protein levels normalized to actin loading at the end of the developmental decrease in REM sleep (day 30) were  $\sim 1/3$  of those at day 10, the beginning of that decrease. Figure 3*E* shows representative Western blots of these results. Pooled samples from four litters showed that Cx 36 protein levels at 10 days (mean  $\pm$  SE of integrated density values,  $17,203 \pm 1,383$ ) versus 30 days ( $4,357 \pm 297$ ) were significantly different (ANOVA,  $df = 7$ ,  $F = 82.48$ ,  $P < 0.001$ ; post hoc Scheffe  $P < 0.05$ ).

#### DISCUSSION

The present study used several techniques to provide evidence for the presence of electrical coupling and neuronal gap junctions within a subset of SubC neurons although each of the lines of research described requires additional investigation. Electrophysiological evidence showed that spikelets were present spontaneously or were induced by CAR, membrane

oscillations and spikelets were induced by CAR in the presence of synaptic blockers, and spikelets and membrane oscillations could be blocked by the putative gap junction blocker CBX. Molecular evidence indicated the presence of both Cx 36 gene expression and protein in the SubC. Our data showed a decrease in Cx36 protein levels that paralleled the developmental decrease in REM sleep.

Although some SubC cells showed spontaneous spikelets, others required the addition of CAR. Others showed dye coupling but only some manifested spontaneous spikelets. Evidently, the conditions under which gap junctions open to produce coupling in the SubC are unknown, which lead us to suspect that we may be underestimating the degree of coupling observed with our current methods. Considering the high levels of Cx 36 gene expression and protein found, especially early in development, electrical coupling may be more prevalent.

The induction of spikelets and membrane oscillations by CAR are similar to those induced in electrically coupled neurons in the hippocampus (Valiante et al. 1995). In fact, these oscillations occurred at a similar frequency to those manifested in the hippocampus, which can generate its own theta frequency in the absence of synaptic inputs (Reich et al. 2005). The observation that CAR induced these effects in the presence of synaptic blockers is good evidence for the presence of electrical coupling as the likely mechanism mediating these oscillations and spikelets. The fact that CBX could block or reduce the occurrence of such oscillations and spikelets (and decreased theta power) further suggests the presence of electrical coupling, although additional testing with more specific gap junction blockers is needed (Cruikshank et al. 2004).

Additional studies are needed to determine if pairs of SubC neurons are directly coupled (we did not record from a pair of directly coupled cells), if the coupled neurons represent specific morphological or transmitter type(s) (ongoing studies are attempting to reconstruct recorded cells and to identify the transmitter type, see following text), and if CAR can increase the degree of dye coupling (fixation immediately after induction of oscillations and spikelets has not been carried out). Future studies will need to address the possibility that some SubC neurons may contact locus coeruleus dendrites, which are known to be electrically coupled.

The observation of significant levels of Cx 36 gene expression and protein levels suggests that this neuronal gap junction protein is active in the mesopontine tegmentum, although its levels show a developmental decrease. Because other regions known to have electrical coupling (locus coeruleus, substantia nigra) were included in these samples, we used punches of the SubC to show the presence of Cx 36 protein. In both cases, the levels of Cx 36 decreased during development, but Cx 36 mRNA and protein levels were still detectable in the adult. This decrease paralleled the developmental decrease in REM sleep, making electrical coupling an attractive candidate mechanism for at least partially explaining the developmental decrement in REM sleep. Additional studies will be needed to establish a stronger link between physiological indices of electrical coupling and levels of Cx 36 mRNA and protein by recording larger numbers of neurons at 10 and 30 days of age (only younger ages were sampled electrophysiologically).

In the cortex, hippocampus and reticular nucleus of the thalamus, networks of electrically coupled neurons appear to be GABAergic (Amitai et al. 2002; Bierlein et al. 2000;

Fukuda and Kosaka 2000; Landisman et al. 2002). The localization of the recorded neurons in the SubC in this study was done using Lucifer yellow diffusion in patched cells and neurobiotin injection and Texas Red immunocytochemistry in sharp electrode cells. We are in the process of determining if all or only some of the neurons described here were GABAergic. On the other hand, a series of studies have shown that cells in the SubC P-wave generating region are immunopositive for vGlut-2 antibody, indicating they are glutamatergic (Datta 2006). It has previously been demonstrated that cholinergic stimulation of the SunC increased glutamate release in the dorsal hippocampus, a site where SubC cells appear to project (Datta 2006).

The present study provides evidence for the presence of functional gap junctions within the SubC nucleus, which has been implicated in the modulation of REM sleep. If electrical synapses are involved in coordinating SubC cells to produce synchrony within this nucleus, they are likely to have a profound effect on the production of PGO waves and will likely have an important role in REM sleep.

#### ACKNOWLEDGMENTS

Present address of Y.-H. Zhou, Dept. of Neurological Surgery, University of California, Irvine, CA.

#### GRANTS

This work was supported by National Institutes of Health Grants NS-20246, DC-06356, DC-07123, and RR-20146.

#### REFERENCES

- Amitai Y, Gibson JR, Beierlein M, Patrick SL, Ho AM, Connors BW, Golomb D.** The spatial dimensions of electrically coupled networks of interneurons in the neocortex. *J Neurosci* 22: 4142–4152, 2002.
- Baghdoyan HB, Rodrigo-Angulo RW, McCarley RW, Hobson JA.** Site-specific enhancement and suppression of desynchronized sleep signs following cholinergic stimulation of three brain stem regions. *Brain Res* 306: 39–52, 1984.
- Beierlein M, Gibson JR, Connors BW.** A network of electrically coupled interneurons drives synchronized inhibition in neocortex. *Nat Neurosci* 3: 904–910, 2000.
- Brown RE, Winston S, Basheer R, Thakkar MM, McCarley RW.** Electrophysiological characterization of neurons in the dorsolateral pontine rapid-eye-movement sleep induction zone of the rat: intrinsic membrane properties and responses to carbachol and orexins. *Neuroscience* 143: 739–755, 2006.
- Connors BW, Long MA.** Electrical synapses in the mammalian brain. *Annu Rev Neurosci* 27: 393–418, 2004.
- Cruikshank SJ, Hopperstad M, Younger M, Connors BW, Spray DC, Srinivas M.** Potent block of Cx36 and Cx50 gap junction channels by mefloquine. *Proc Natl Acad Sci USA* 101: 12364–12369, 2004.
- Datta S.** Activation of phasic pontine-wave generator: a mechanism for sleep-dependent memory processing. *Sleep Biol Rhythms* 4: 16–26, 2006.
- Datta S, Siwek DF.** Single cell activity patterns of pdunculopontine tegmentum neurons across the sleep-wake cycle in the freely moving rats. *J Neurosci Res* 70: 611–621, 2002.
- Datta S, Siwek DF, Patterson EH, Cipollini PB.** Localization of pontine PGO wave generation sites and their anatomical projections in the rat. *Synapse* 30: 409–423, 1998.
- Deurveilher S, Hennevin E.** Lesions of the pedunculopontine tegmental nucleus reduce paradoxical sleep (PS) propensity: evidence from a short-term PS deprivation study in rats. *Eur J Neurosci* 13: 1963–1976, 2001.
- Fukuda T, Kosaka T.** Gap junctions linking the dendritic network of GABAergic interneurons in the hippocampus. *J Neurosci* 20: 1519–1528, 2000.
- Garcia-Rill E, Kobayashi T, Good C.** The developmental decrease in REM sleep. *Thal Related Syst* 2: 115–131, 2003.
- Gerber U, Stevens DR, McCarley RW, Greene RW.** Muscarinic agonists activate an inwardly rectifying potassium conductance in medial pontine

- reticular formation neurons of the rat in vitro. *J Neurosci* 11: 3861–3867, 1991.
- Greene RW, Gerber U, McCarley RW.** Cholinergic activation of medial pontine reticular formation neurons in vitro. *Brain Res* 476: 154–159, 1989.
- Imon H, Ito K, Dauphin L, McCarley RW.** Electrical stimulation of the cholinergic laterodorsal tegmental nucleus elicits scopolamine-sensitive excitatory postsynaptic potentials in medial pontine reticular formation neurons. *Neuroscience* 74: 393–401, 1996.
- Iruthayanathan M, Zhou YH, Childs GV.** Dehydroepiandrosterone restoration of growth hormone gene expression in aging female rats, in vivo and in vitro: evidence for actions via estrogen receptors. *Endocrinology* 146: 5176–87, 2005.
- Jouvet M, Delorme F.** Locus coeruleus et sommeil paradoxal. *C R Soc Biol Paris* 159: 895–899, 1965.
- Jouvet-Mounier D, Astic L, Lacote D.** Ontogenesis of the states of sleep in rat, cat, and guinea pig during the first postnatal month. *Dev Psychobiol* 2: 216–239, 1970.
- Karlsson KA, Gall AJ, Mohns EJ, Seelke AM, Blumberg MS.** The neural substrates of infant sleep in rats. *PLoS Biol* 3:e143, 2005.
- Landisman CE, Long MA, Beierlein M, Deans MR, Paul DL, Connors BW.** Electrical synapses in the thalamic reticular nucleus. *J Neurosci* 22: 1002–1009, 2002.
- Lu J, Sherman D, Devor M, Saper CB.** A putative flip-flop switch for control of REM sleep. *Nature* 441: 589–594, 2006.
- Marks GA, Farber J, Roffwarg HP.** Metencephalic localization of ponto-geniculo-occipital waves in the albino rat. *Exp Neurol* 69: 667–677, 1980.
- Mavanji V, Ulloor J, Saha S, Datta S.** Neurotoxic lesions of phasic pontine-wave generator cells impair retention of 2-way active avoidance memory. *Sleep* 27: 1282–1292, 2004.
- Mitani A, Ito K, Hallanger AE, Wainer BH, Kataoka K, McCarley RW.** Cholinergic projections from the laterodorsal and pedunculopontine tegmental field to the pontine gigantocellular tegmental field in the cat. *Brain Res* 451: 397–402, 1988.
- Mitler MM, Dement WC.** Cataleptic-like behavior in cats after microinjections of carbachol in pontine reticular formation. *Brain Res* 68: 335–343, 1974.
- Morrison AR.** Paradoxical sleep without atonia. *Arch Ital Biol* 126: 275–289, 1988.
- Moruzzi G, Magoun HW.** Brain stem reticular formation and activation of the EEG. *Electroencephalogr Clin Neurophysiol* 1: 455–473, 1949.
- Mouret J, Delorme F, Jouvet M.** Lesions of the pontine tegmentum and sleep in rats. *CR Seances Soc Biol Fil* 161: 1603–1606, 1967.
- Reese NB, Garcia-Rill E, Skinner RD.** The pedunculopontine nucleus-auditory input, arousal and pathophysiology. *Prog Neurobiol* 47: 105–133, 1995.
- Reich CG, Karson MA, Karnup SV, Jones LM, Alger BE.** Regulation of IPSP theta rhythm by muscarinic receptors and endocannabinoids in hippocampus. *J Neurophysiol* 94: 4290–4299, 2005.
- Roffwarg HP, Muzio JN, Dement WC.** Ontogenetic development of the human sleep-dream cycle. *Science* 152: 604–619, 1966.
- Sakai K, El Mansari M, Jouvet M.** Inhibition by carbachol microinjections of presumptive cholinergic PGO-on neurons in freely moving cats. *Brain Res* 527: 213–223, 1990.
- Sanford LD, Morrison AR, Graziella LM, Harris JS, Yoo L, Ross RJ.** Sleep patterning and behavior in cats with pontine lesions creating REM without atonia. *J Sleep Res* 3: 233–240, 1994.
- Shiromani P, Armstrong DM, Gillin JC.** Cholinergic neurons from the dorsolateral pons project to the medial pons: a WGA-HRP and choline acetyltransferase immunohistochemical study. *Neurosci Lett* 95: 12–23, 1988.
- Srinivas M, Rozental R, Kojima T, Dermietzel R, Mehler M.** Functional properties of channels formed by the neuronal gap junction protein connexin 36. *J Neurosci* 19: 9848–9855, 1999.
- Stevens DR, Birnstiel S, Gerber U, McCarley RW, Greene RW.** Nicotinic depolarizations of rat medial pontine reticular neurons studied in vitro. *Neuroscience* 57: 419–424, 1993.
- Steriade M, Datta S, Pare D, Oakson G, Curro Dossi R.** Neuronal activities in brain-stem cholinergic nuclei related to tonic activation processes in thalamocortical systems. *J Neurosci* 10: 2541–2559, 1990a.
- Steriade M, Paré D, Datta S, Oakson G, Curro Dossi R.** Different cellular types in mesopontine cholinergic nuclei related to ponto-geniculo-occipital waves. *J Neurosci* 10: 2560–2579, 1990b.
- Valiante TA, Perez JL, Velazquez J, Jahromi SS, Carlen PL.** Coupling potentials in CA1 neurons during calcium-free-induced field burst activity. *J Neurosci* 15: 6946–56, 1995.
- Vandecasteele M, Glowinski J, Venance L.** Electrical synapses between dopaminergic neurons of the substantia nigra pars compacta. *J Neurosci* 25: 291–298, 2005.
- Vanni-Mercier G, Debilly G.** A key role for the caudoventral pontine tegmentum in the simultaneous generation of eyesaccades in bursts and associated ponto-geniculo-occipital waves during paradoxical sleep in the cat. *Neuroscience* 86: 571–585, 1989.
- Veruki ML, Hartveit E.** Electrical synapses mediate signal transmission in the rod pathway of the mammalian retina. *J Neurosci* 22: 10558–10566, 2002.
- Walton KD, Navarrete R.** Postnatal changes in motoneurone electrotonic coupling studied in the in vitro rat lumbar spinal cord. *J Physiol* 433: 283–305, 1991.
- Webster H, Jones BE.** Neurotoxic lesions of the dorsolateral pontomesencephalic tegmentum-cholinergic cell area in the cat.II. Effects upon sleep-waking states. *Brain Res* 458: 285–302, 1988.
- Yamamoto K, Mamelak AN, Quattrochi JJ, Hobson JA.** A cholinergic desynchronized sleep induction zone in the anterolateral pontine tegmentum: locus of the sensitive region. *Neurosci* 39: 279–293, 1990.
- Zhou YH, Hess RK, Liu L, Linskey ME, Yung WKA.** Modeling prognosis for patients with malignant astrocytic gliomas: quantifying the expression of multiple genetic markers and clinical variables. *Neurooncology* 7: 485–94, 2005.
- Zhou YH, Tan F, Hess KR, Yung WK.** The expression of PAX6, PTEN, vascular endothelial growth factor, and epidermal growth factor receptor in gliomas: relationship to tumor grade and survival. *Clin Cancer Res* 9: 3369–75, 2003.